

II. Non-commuting Matrix Solution of DGLAP; $F_2^{p,d}$ Data Leading to Partons Directly without Parameterization

M. Goshtasbpour¹, and M. Zandi²

¹ *Dept. of Physics, Shahid Beheshti University, G. C., Evin 19834, Tehran, Iran.*

² *II. Physikalisches Institut Georg August Universität Göttingen, Germany.*

Dominant present path for determination of parton distribution functions (pdfs) from data is based on pre-assumed form of parametric pdfs. Here, an alternative direct, or non-parametric method of pdf extraction is spelled out. As the main task, least square estimates of the central values of pdfs are obtained at a chosen Q^2 , and at $x_i, i = 1, \dots, n$ of the analyzed $F_2^{p,d}$ data points. In the process, numerically singular system of LO PQCD weighted linear combination of decomposition equations of the data points, each at a given $(x_i, Q_{ij}^2), j = 1, \dots, n_i$, obtained from a respective χ^2 , together with the equations of ZM VFN constraints, are solved. In each data equation, the corresponding data points are decomposed into their pdf components, evolved from the set of unknown pdfs at $(x_i, Q^2), i = 1, \dots, n$. A similar evolution is done in the constraints. As a complementary task, the constrained discretization of Bjorken x , required for the commuting solution of DGLAP, [1], is relaxed, and a non-commuting solution on the more natural set of exact x -points of the data is developed.

PACS numbers: 12.38.Bx

INTRODUCTION

Decomposition equation of each data point serves as a weighted component of data equations on parton distribution functions (pdfs), and each ZM VFN constraint is a theoretical equation on pdfs, at different Q^2 of the data and constraints, at a given order in PQCD. The integro-differential DGLAP evolution equations of the same order in perturbation may then be solved and used to bring all the pdfs to the unique Q^2 of the unknowns in the resulting numerically singular system of linear equations to be solved (via SVD). Here, in the second paper of the series, the process is realized, for the simplest example, on $F_2^{p,d}$ data at leading order (LO), with possible wider implications.

NON-COMMUTING SOLUTIONS OF ALL DGLAP EQUATIONS

In contrast to commuting solutions of DGLAP equations, [1], with commuting banded (bdd) lower triangular (l.t.) splitting function matrices, here, more general non-commuting solutions of DGLAP equations, with non-commuting, non-bdd l.t. splitting function matrices are considered because of their advantage in data analysis.

n Dimensional x -Space of Data Points and each pdf Set

Referring to the corresponding section in [1], commuting solutions of DGLAP constrain the discrete x -basis, for the linear algebra, to be of the form

$$x_i = x_1^i, \quad i = 1, \dots, n, \quad (1)$$

in order to have commuting banded (bdd) lower triangular (l.t.) splitting function matrices. Discrete x in (1) are not the exact x -points of the data. So, eventually, for data analysis, interpolation techniques should be used.

The non-commuting numerical solutions, to be presented in this section, can simply use the exact Bjorken $x = \{x_i, i = 1, \dots, n\}$ of the data set. On either discrete x -set, a discrete set of n basis vectors for each pdf set is defineable. Thus, the splitting functions operating on this basis (space) can be calculated as $n \times n$ matrices.

Flavor Evolution Equation

At LO, where equality of splitting functions (neglecting quark masses), leaves only four different ones, the evolution equation can be written in the simple form of $(m + 1)$ coupled equations of m independent quarks and

antiquarks coupled through gluon distribution, (2).

$$\frac{\partial}{\partial t} \begin{pmatrix} q_1(x, t) \\ \vdots \\ q_m(x, t) \\ g(x, t) \end{pmatrix} = \int_x^1 \frac{dy}{y} \begin{pmatrix} P_{qq}(\frac{x}{y}) & 0 & \cdots & 0 & P_{qg}(\frac{x}{y}) \\ 0 & \ddots & \ddots & \vdots & \vdots \\ \vdots & \ddots & \ddots & 0 & \vdots \\ 0 & \cdots & 0 & P_{qq}(\frac{x}{y}) & P_{qg}(\frac{x}{y}) \\ P_{gq}(\frac{x}{y}) & \cdots & \cdots & P_{gq}(\frac{x}{y}) & P_{gg}(\frac{x}{y}) \end{pmatrix} \cdot \begin{pmatrix} q_1(y, t) \\ \vdots \\ q^{(m)}(y, t) \\ g(y, t) \end{pmatrix} \quad (2)$$

where

$$\frac{dt}{d\text{Ln}(Q^2)} = \frac{\alpha_s(Q^2)}{2\pi}. \quad (3)$$

For n_f flavors, However, usually, a linear combination, may reduce m and modify coefficient of P_{qg} , e.g., $m \rightarrow 2n_f - 2$ for FIG. 1 of [1], for use of total c and b pdfs; or $m \rightarrow n_f$ in the $F_2^{p,d}$ data analysis, in the present paper, due to use of q_{total} for all the flavors.

Flavor evolution DGLAP (2) is considered as an alternative to *non-singlet*, *singlet* ($NS - S$) division of DGLAP already discussed in [1]. Thus, both have the same number of independent parton distributions. Here, FIG. 1 to FIG. 6 show the $(n_F + 1)$ resulting pdfs of our $F_2^{p,d}$ data analysis.

Similar to the case of *singlet*, [1], as all the kernels are t independent, we expect the solution for finite Q^2 interval to be of the form:

$$f^F(t) = e^{(t-t_0)P_F} f^F(t_0), \quad (4)$$

where f^F , is a $(m+1)$ column vector of quarks and gluon and P_F is the kernel of (2) respectively.

The *singlet* and the *flavor* kernels have some essential similarities that help in finding the analytic commuting solution of the *flavor* DGLAP for finite Q^2 interval. The result may be presented in a future paper. For the present, we can have the numerical non-commuting solutions of FIG. 1 to FIG. 6.

Numerical Non-commuting Solutions for Finite Q^2 Interval for all forms of DGLAP Equations

Here, based on the exact Bjorken x_i of data points, e.g. for the structure functions, numerical non-commuting solution of the DGLAP equations is presented. DGLAP equations are of the generic form:

$$\frac{df_K(x, t)}{dt} = \int_x^1 \frac{dy}{y} P^K(\frac{x}{y}) f_K(y, t), \quad (5)$$

where K can be NS, S , or F . Having the matrix forms of the splitting functions kernels, section (2), matrix forms of the DGLAP equations are:

$$\frac{df_i^K(t)}{dt} = \sum_{j=1}^i P^K_{ij} f_j^K(t) \Leftrightarrow \frac{d\mathbf{f}^K(t)}{dt} = \mathbf{P}^K \cdot \mathbf{f}^K(t). \quad (6)$$

Independence of the kernels from the variable t , leads the following solution to equation (6), for the finite evolution from t_0 to t .

$$\mathbf{f}^K(t) = e^{(t-t_0)\mathbf{P}^K} \cdot \mathbf{f}^K(t_0) \equiv \mathbf{E}^K(t-t_0) \cdot \mathbf{f}^K(t_0). \quad (7)$$

The final $(t-t_0)$ dependent \mathbf{E}^K matrix constitutes the essential solution of DGLAP equations for finite evolution.

To determine the matrix form of $\mathbf{E}^K(t-t_0) = e^{(t-t_0)\mathbf{P}^K}$, the choice of (1) is mandatory to have commuting, banded triangular, splitting functions matrices, for a finite expansion of the exponential in the analytical commuting solution of (7), [1, 2]. But experimental data points do not exactly match the x points of (1). So, eventually, interpolation techniques should be used.

However, as hinted below equation (1), such restrictions is not necessary. Exponential of the non-banded (non-commuting) form of the LO kernels P_{NS}, P_S and P_F can be numerically calculated, for the non-commuting solution of (7), at least within our limited data analysis. Using numerical algorithms to approximate the exponential in (7) brings freedom from banded triangular matrices, so one could use experimental x points directly to discretize the x space.

In this paper, we go directly to the non-commutative solutions, based on the sequence of x points of data, aimed at $F_2^{p,d}$ data analysis for finding NS, S , and g pdfs. The question of comparison with flavor solutions can (may?) be trivial, considering prevailing linearity, or (massless) $SU(n_F)$, $n_F \leq 5$ symmetry, or our ZM VFN constraints, discussed in the next section. It is also computationally tested via indirect flavor evolution of [1].

INTRODUCTION TO DATA ANALYSIS OF STRUCTURE FUNCTIONS $F_2^{p,d}$

LO decomposition equation (factorization) of F_2 is:

$$F_2 = x(1 + \frac{\alpha_s}{2\pi} C_q) \otimes \hat{F}_2^q + x \frac{\alpha_s}{2\pi} C_g \otimes (\sum_F e_F^2) g, \quad (8)$$

with the quark structure function in term of $n_F = 5$ flavors $NS - S$, with usual definitions for p and d

$$\hat{F}_2^{q/p} = \frac{1}{90} (22\Sigma + 3q^{(24)} - 5q^{(15)} + 5q^{(8)} + 15q^{(3)}), \quad (9)$$

$$\hat{F}_2^{q/d} = \frac{\hat{F}_2^{q/p} + \hat{F}_2^{q/n}}{2} = \frac{1}{90} (22\Sigma + 3q^{(24)} - 5q^{(15)} + 5q^{(8)}).$$

The simplest choice we have made by writing (9), unrealistically with $SU_F(5)$ symmetry, needs explanation.

Within a VFN point of view, if it was not for bringing in some minimal mass effects of heavy quarks c and b , QED DIS would be limited to three light quarks. Why so? Because zero-mass assumption for the three lightest quarks is well justified, $m_q^2 \ll Q^2$, Q^2 in the whole range of data and simulation. There is the possibility of differentiating square of electric charge, e_q^2 at γ^* quark vertex in proton or deuteron DIS, so u_{total} stands apart. Isospin symmetry differentiates d_{total} and s_{total} . In other words, detection of electric charge squared weight of q_{total} may leave us two quarks in form of a singlet q^S , and a non-singlet q^{NS} , and isospin symmetry differentiates data and the set of variables $q^3 \propto F_2^{(p-d)}$ from q^{NS} which now becomes q^8 , the $SU_F(3)$ octet. In this sense, could we say there is something of an $SU_F(3)$ symmetry?

It is trivial that $F_2^{p,d}$ have no information on the non-singlet valence quarks. Thus, pdfs are extracted from $F_2^{p,d}$ as total: sea and valence are not separable.

Bringing in minimal mass effects of heavy quarks, c and b , to the measured data points, $F_2^p(x_{ij}, Q_j^2)$ and $F_2^d(x_{ij}, Q_j^2)$, in different regions of Q^2 , corresponding to 4, and 5 flavors, allows unveiling of the 4th and 5th flavors. $SU_F(3) \rightarrow SU_F(5)$ symmetry under the assumption of having five zero-mass flavors symmetrically, as unrealistic or highly errored, as a simple ZM VFN scheme may be.

Under $SU_F(5)$, differentiation of q^{15} and q^{24} once again leaves $q^{NS} = q^8$ as it was. Thus, two additional sets of nonsinglet degrees of freedom are brought in q_{n-1} with addition of the n th quark as a heavy flavor as Q^2 increases. Finally, the number of extractable pdf central value sets increases to $n_F + 1$. The additional one pdf is the gluon of gluon vertex.

Simulation of our direct method is a testing ground for this point of view, its correction and refinement. Investigation of deviation from $SU_F(5)$ symmetry in the well-known regions of Q^2 , is left out to be dealt with soon.

Minimal mass effects, at masses of c and of b quarks, for us, are continuity constraints $c(Q^2 = m_c^2) = 0$, and $b(Q^2 = m_b^2) = 0$ at Bjorken $x = \{x_i, i = 1, \dots, n\}$ of the data set, at the boundary between regions of Q^2 where it is assumed that n_F respectively crosses 3 to 4, and 4 to 5 flavors. In other words, constraints equate the singlet, Σ , and the $(n_F^2 - 1)$ -multiplet (NS) of the $SU(n_F)$ flavor symmetry of the region above each boundary; thus, dropping the flavor number, n_F , by 1 at and below the boundary. The constraint equations, together with consistent evolution, keep the continuity of the pdfs while the flavor numbers change at the boundary.

Along with continuity of pdfs, we have continuity for the coupling constant as a changing Q^2 crosses massive quark m_b^2 .

Positions of $Q^2 = m_b^2$ is in practice very different from

$Q^2 = m_c^2$. $Q^2 = m_c^2$ lies asymptotically outside the Q^2 range, as equations of BCDMS data, [3], are simulated here. It is only for b that a break takes place when evolution between the data and our simulation crosses $Q^2 = m_b^2$. Then, solving DGLAP for finite evolution $[Q_j^2, Q^2]$ is divided into two stages of $[Q_j^2, m_b^2]$ and $[m_b^2, Q^2]$. Furthermore, there are two sets of inputs, the first set has $n_f = 4$ flavors at Q_j^2 , the second set has ($n_f = 5$) flavors at m_b^2 . In addition, the second set of inputs is the first set of outputs with an extra input pdf for the heavy quark, $b(Q^2 = m_b^2) \equiv 0$, our minimal effect of mass of $b!$ In order to carry out the comparison with MSTW, we take their value, $m_b = 4.75 \text{ Gev}$ [4].

In the direct, non-parametric, data analysis of DIS, a singular system of linear equations of data and VFN constraints is encountered. Direct pdf variables of this method are a few times more (next section), also in [5], than the number of parameters of the parametric data analysis. A very simple idealization, a ZM-VFN scheme employed via the constraint equations, brought the first successful removal of singularity via SVD. It is presented in its simplicity here, before further realistic elaborations of the effects of heavy quarks masses. In a coming step, a critique, including that of the massless coefficient functions, (10) and (12), having large errors, is to be done.

Example Calculation of Coefficient Function Matrices

The kernel of the convolutions, in DIS data analysis, is either the splitting functions for DGLAP, or the coefficient functions of the hadronic structure function, e.g. (8). Construction of the matrix coefficient functions, for DIS, follows closely the path of construction of splitting functions, resulting in either commuting, banded lower triangular, or noncommuting matrices, respectively, only depending upon whether equation (1) is followed for discretization of x or not. The two possibilities lead to analytical, [1], or more general numerical approaches.

With examples on splitting functions, derivation of P_{qq} was spelled out in [1]. In a second example calculation, the matrix form of the LO \overline{MS} coefficient functions $C_q(x)$ and $C_g(x)$, suited for our ZM VFN scheme, are derived here, beginning with [6]:

$$C_q(z) = \frac{4}{3} \left[2 \left(\frac{\ln(1-z)}{1-z} \right)_+ - \frac{3}{2} \left(\frac{1}{1-z} \right)_+ - (1+z) \times \right. \\ \left. \ln(1-z) - \frac{1+z^2}{1-z} \ln z + 3 + 2z - \left(\frac{\pi^2}{3} + \frac{9}{2} \right) \delta(1-z) \right]. \quad (10)$$

Using definition of "+" regularization, integrating $C \otimes \hat{F}_2^q$, (8), by parts, in which $dv_1 = \frac{8}{3} \frac{\ln(1-y)}{1-y} dy$, and $dv_2 = \frac{4}{3} [-(1+y) \ln(1-y) - \frac{1+y^2}{1-y} \ln y + 3 + 2y] dy$; the matrix of coefficients of n -tuple q may be read as:

$$C_q : \begin{cases} (C_q)_{ii} = a + \frac{1}{x_i - x_{i-1}} \int_{x_i}^{x_{i-1}} \{v_1(\frac{x_i}{y}) + v_2(\frac{x_i}{y})\} dy \\ (C_q)_{ik} = \frac{1}{x_k - x_{k-1}} \int_{x_k}^{x_{k-1}} dy \{v_1(\frac{x_i}{y}) + v_2(\frac{x_i}{y})\} \\ v_2(\frac{x_i}{y}) - \frac{1}{x_{k+1} - x_k} \int_{x_{k+1}}^{x_k} dy \{v_1(\frac{x_i}{y}) + v_2(\frac{x_i}{y})\}. \end{cases} \quad (11)$$

where $a = v_2(1) - v_1(0) - 4\pi^2/9 - 6$.

Similarly for $C_g(x)$, beginning with [6]:

$$C_g(z) = \frac{1}{2} [((1-z^2) + z^2) \ln(\frac{1-z}{z}) - 8z^2 + 8z - 1], \quad (12)$$

we will get the matrix form:

$$C_g : \begin{cases} (C_g)_{ii} = v(1) + \frac{1}{x_i - x_{i-1}} \int_{x_i}^{x_{i-1}} v(\frac{x_i}{y}) dy \\ (C_g)_{ik} = \frac{1}{x_k - x_{k-1}} \int_{x_k}^{x_{k-1}} v(\frac{x_i}{y}) dy - \\ \frac{1}{x_{k+1} - x_k} \int_{x_{k+1}}^{x_k} v(\frac{x_i}{y}) dy \end{cases} \quad (13)$$

where $dv = C_g(y)dy$.

EXTRACTION OF LEAST SQUARE ESTIMATES OF THE CENTRAL VALUES OF PDFS FROM $F_2^{p,d}$ DATA AND THEIR COMPARISON WITH MSTW PDFS

At this stage, we are ready, with a bare minimum required for SVD to work, to get the central values of pdfs from $F_2^{p,d}$ data. For the numerical solution, each $F_2^{p,d}$ data point at a given (x_i, Q_i^2) of an experiment, e.g BCDMS [3], is decomposed into its partonic components via (8) and (9), evolved by our solutions of DGLAP, from a set of unknown pdfs, $u_k, k = 1, \dots, m = (n_F + 1) \times n - 1$,* at $(x_i, Q^2), i = 1, \dots, n$, with a chosen Q^2 .

The linear system of m data equations and $(2n - 1)$ ZM VFN constraints may be denoted as:

$$A_{ij}u_j = b_i, i = 1, \dots, m + (2n - 1), j = 1, \dots, m, \quad (14)$$

where the data equations come from minimization of χ^2 :

$$\chi^2 = \sum_{ij} \frac{(F_{2ij}^L - F_{2ij}^R)^2}{\sigma_{ij}^2}, \quad (15)$$

with respect to the unknowns,

$$\frac{\partial \chi^2}{\partial u_k} = 0, k = 1, \dots, m. \quad (16)$$

F_{2ij}^L is the value of data point on the left side of (8), with σ_{ij} its quadratically calculated total error, and F_{2ij}^R its LO decomposition corresponding to the right side of (8, 9). In (15), for data sets such as BCDMS [3], a sum over proton and deuteron data points is understood.

The cut on data is set, in principle, to separate the Q^2 regions of PQCD and higher twists at the invariant mass squared $W^2 = 20 \text{ Gev}^2$, similar to MSTW LO cuts, [4, 5]. Number of proton and deuteron data points used are 153 and 146 respectively, thus less than 4% of the total BCDMS [3] data is cut out. Ability to utilize correct cuts is a major improvement of the present version of the paper. It will be further discussed in [5].

Least square estimates of the central values of unknown pdfs $u_k, k = 1, \dots, m$, at the chosen Q^2 , are obtained by solving the numerically singular system of linear equations (14) of the data, and ZM VFN constraints. Singular value decomposition (SVD) is the essential tool for bringing out the physically acceptable solutions from the context of singularity. In [5] there will be extended exposition of the workings of SVD. Here, is how we learned to use SVD.

Matrix of the coefficients A in (14) is singular. SVD helps separating and managing the singularity, namely the null subspace of the linear space of the singular matrix [7]. The magic of SVD here is to pinpoint numerically too small, deletable, eigenvalues, corresponding to a deletable set of eigenvectors of the numerical null subspace.

Operationally, i.e, in the process of trial motion up or down an indicator of the scale of ordered eigenvalues in the simulation program, there is a single physical criterion for uncovering the border of null subspace, or the place (the indicator value) of its largest eigenvalue: sudden appearance of well patterned, physically acceptable, set of solutions of the linear system, here the LS estimates of every pdf set, which takes place along with the deletion of the corresponding null subspace.** We'll be using this concept as the **first** characterization or "qualitative, intuitive, physical definition" of null subspace of a singular matrix, developed quantitatively in [5].

Results

The results are presented in the first six figures, with similar graphic symbols (described in the 1st legend), at two values of $Q^2 = 37.5$ and 1000 Gev^2 , at which solutions are computed independently, and then compared with MSTW. The first Q^2 is chosen near the center of population of the data points, in the non-asymptotic area

of our ZM VFN in conflict with GM VFN of MSTW; the second is in the deep asymptotic area. FIG. 1 shows the SU(5) singlet, the most exact of the directly extracted pdf points from $F_2^{p,d}$ data point. FIG. 2 shows the five flavor gluon, the least exact of the extracted pdfs points.

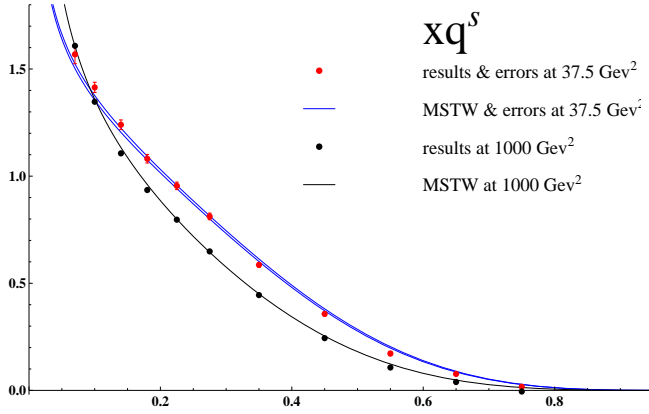


FIG. 1. Points of the SU(5) singlet pdf at the x -points of the BCDMS $F_2^{p,d}$ data from which they are extracted, in comparison with MSTW's. The choices of $Q^2 = 37.5$ and 1000 GeV^2 of the graphs are arbitrary. The first is chosen near the center of population of the data points, in the non-asymptotic area of our ZM VFN in conflict with GM VFN of MSTW. The second is in the deep asymptotic area. The error analysis is done in [5]. This is the most exact of the directly extracted pdf points from $F_2^{p,d}$ data point.

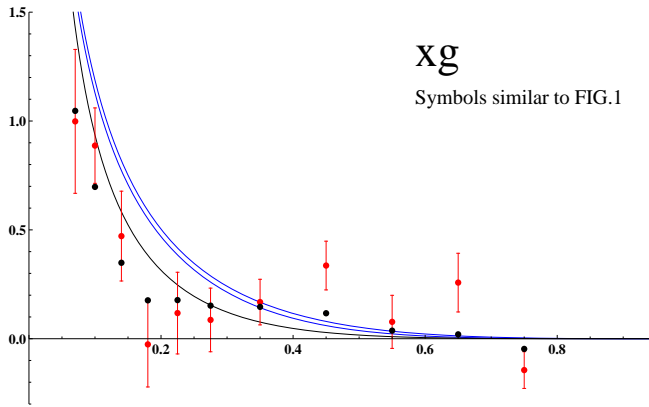


FIG. 2. Gluon; graphic symbols and caption similar to those of FIG. 1. This is the least exact of the extracted pdfs points. Partially, smoothed at $Q^2 = 1000 \text{ GeV}^2$ due to larger intervals of evolution.

Choosing $Q^2 = 1000$ well in the asymptotic region will not improve the observable lower large- x , and higher small- x mismatch with respect to MSTW, but smoothens out the gluon and the NS pdfs (except q_3 because of its independence) due to larger intervals of evolution, taking place while setting up equations (16). before obtaining the SVD solutions.

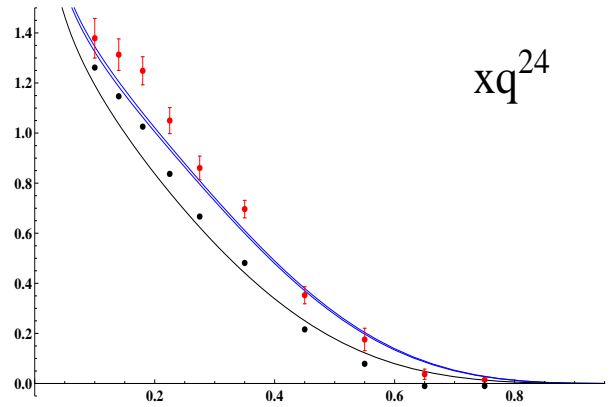


FIG. 3. NS pdf xq^{24} . Graphic symbols and caption similar to those of FIG. 1. There is an observable large- x small- x mismatch with MSTW as described in the text, common to all NS pdfs.

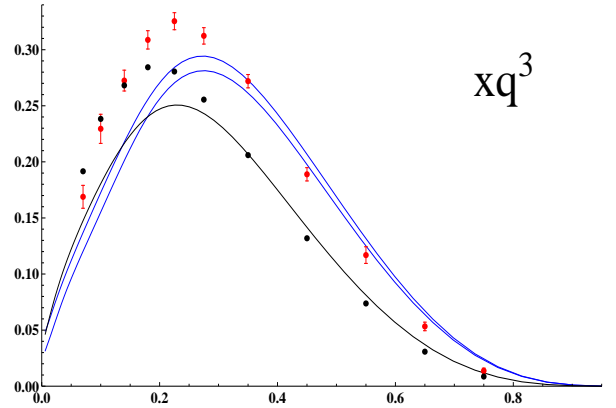


FIG. 4. Independent (in the sense of text in "Discussion") NS pdf xq^3 . Caption similar to that of FIG. 3.

Discussion and prospects

The lower large- x , and higher small- x mismatch with respect to MSTW, pronounced in all NS pdfs, seems to come out of an x -dependent convolution found in factorizations. Thus we may have a clue where to search for it.

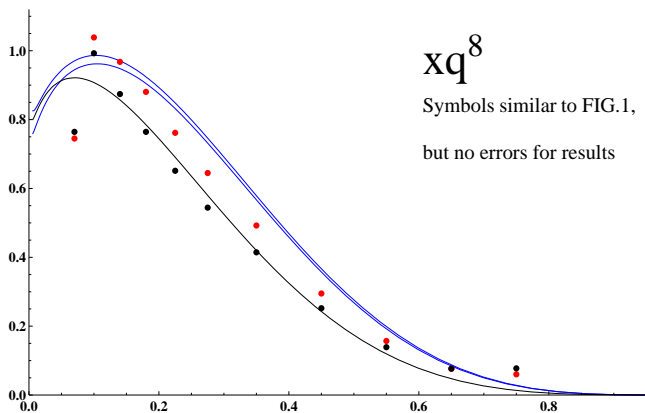


FIG. 5. NS pdf xq^8 . Caption similar to that of FIG. 3. Errors and their discussion is left to [5].

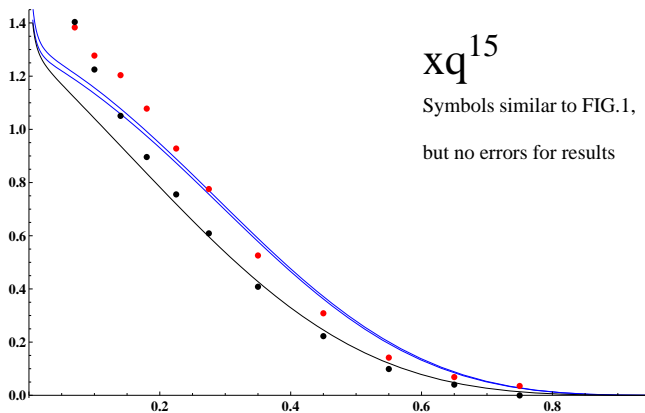


FIG. 6. NS pdf xq^{15} . Caption similar to that of FIG. 3. Errors and their discussion is left to [5].

First of all, we intend to remedy the very simple ZM VFN constraints (scheme), entering abruptly at the boundaries $Q^2 = m_{c,b}^2$. This is to be done after the present paper.

Here attention is drawn to the following computational test of the theoretical necessity of having our c quark constraints as a possible minimum mass effect for having $(n_F + 1)$ pdf central values.

At $Q^2 = m_c^2 = 1.96 \text{ GeV}^2$, constraints may not appear to be as crucial as those at $Q^2 = m_b^2$ from a practical point of view. We are in the asymptotic region for c pdf, when working above the minimum of BCDMS data at $Q^2 = 7.5 \text{ GeV}^2$. At m_c^2 , even these constraints are overlapping with the higher twist boundary set at $W^2 = Q^2(1/x - 1) = 20 \text{ GeV}^2$. However, even in that asymptotic Q^2 region, without c constraints, SVD cannot produce physical results, FIG. 7 and FIG. 8, magically (at this stage of understanding) pointing out a deep deficiency in such a practical point of view. Anchorage of the pdf $c(m_c^2) = 0$ sets essential physical constraints towards asymptotic use of our ZM VFN, whether evolution takes

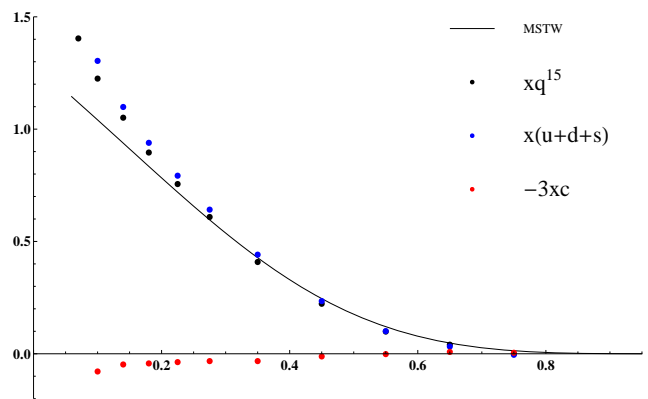


FIG. 7. At $Q^2 = 1000 \text{ GeV}^2$, MSTW (solid line), and our NS pdf q^{15} (11 black dots) and its two, positive ($u + d + s$) and negative ($-3c$), components (10* dots in color each), with both series of c and b constraints. SVD produces acceptable physical results.

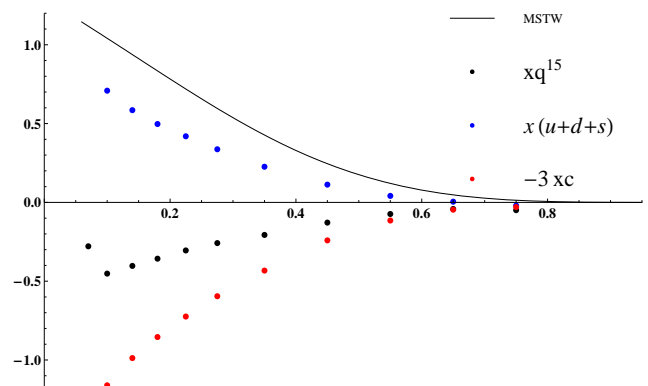


FIG. 8. Here, everything is the same as in FIG. 7, but without the series of c constraints. q^{15} is the most adversely affected pdf from **lack of ZM VFN constraints at $Q^2 = m_c^2$** . Here, SVD cannot produce physical results .

place in the asymptotic region for c pdf or not.

Operating. At, $m_b^2 = 22.5625 \text{ GeV}^2$, in the middle of the finite $\Delta Q^2 = [7.5, 230] \text{ GeV}^2$ interval of BCDMS data, constraints are not only unavoidable in the above sense, but also are practically used in process of evolution through $Q^2 = m_b^2$.

The path towards global data analysis, beginning with electroweak and going to hard scattering, to determine $(2n_F + 1), n_F \rightarrow 6$ Standard Model pdfs is open. Quadratic non-linearity of hard scattering may need due attention.

The path towards higher order analysis seems not only open via the numerical noncommutative solutions to DGLAP presented, but also at least in some cases analytically ; e.g., we have developed an NLO NS commuting solution of DGLAP. Most importantly, A Higher Order Perturbative Parton Evolution Toolkit, HOPPET,

[11], which we became familiar with only very recently, is exactly of the same family as ours, and of great value in this respect.

ACKNOWLEDGEMENTS

Thanks to P. G. Ratcliffe for inception of the idea.

-
- [1] Mehrdad Goshtasbpour and Seyed Ali Shafiei, arXiv: 1303.3985
 - [2] M. Goshtasbpour and P. G. Ratcliffe, 14th International Spin Physics Symposium, Osaka, Japan, Oct. 16-21, 2000, P. 879; P. G. Ratcliffe, *Phys. Rev. D* **63**, 116004 (2001), arXiv: hep-ph/ 0012376; S.A. Shafiei, *A Study of DIS and a Novel Solution to DGLAP Evolution Equation*, M.S. Thesis, Shahid Beheshti University (2002).
 - [3] Benvenuti et al, BCDMS, *Phys. Lett. B* **223**, 485 (1989).
 - [4] A.D. Martin, W.J. Stirling, R.S. Thorne, G. Watt *Eur.Phys.J.* **C63**:189-285 (2009).
 - [5] M. Goshtasbpour, *Singular Value Decomposition, Hessian Errors, and Linear Algebra of Non-parametric Extraction of Partons from DIS*. To be submitted
 - [6] R.K. Ellis, W.J. Stirling, B.R. Webber, *QCD and Collider Physics*, Cambridge university press (1996).
 - [7] Press, W.H., et al., *Numerical Recipes*, Cambridge University Press, 1992.
 - [8] Arneodo, et al., NMC, *Phys. Lett. B* **364**, 107 (1995).
 - [9] Mehrdad Goshtasbpour and Seyed Ali Shafiei, 15th International Spin Physics Symposium, Long Island, N. Y.,

Sept. 9-14, 2002, AIP Conf. Proc. **676**, 299-302 (2003).

Also in "Upton/Danvers 2002, Spin 2002 " 299-302.

- [10] Mohammad Zandi, *A New Numerical Matrix Solution for DGLAP Evolution Equation of PQCD and Application*, M.S. Thesis, Shahid Beheshti University (2010).
- [11] Gavin P. Salam and Joan Rojo, *Comp. Phys. Comm.* **180**, 120 (2009), arXiv:0804.3755.

* Subtraction of one, from the number of unknowns and the corresponding constraint equations, is an indication of lack of information or data on a particular pdf variable, namely, $b(x_{11} = .07)$. In other words, to compare our results with MSTW, we use their constants including $m_b^2 = 22.56 \text{ GeV}^2$, and at $x_{11} = .07$, BCDMS's highest $Q^2 = 19 < 22.56 \text{ GeV}^2$. This leads to a missing point at $x_{11} = .07$ in graphs of the results wherever $b(x_{11} = .07)$ is involved.

**A note on the history of this point. The 3rd reference of [2], has a good overlap with this paper. There, we went as far as decomposing F_2 of NMC [8] with the Commutative Matrix solutions of DGLAP with the best fit of Bjorken x given in Table I of [1], and discovering the singularity of resulting linear system of equations, an obstacle in the way of further development in 2002, [9]. In some years, application of the essential tool, SVD, was learned; trial and error for discovery in phenomenology emerged as a method of work. Eventually, during MZ's master thesis [10], a fine tuning of SVD was achieved and the essential non-singular physically desirable results were brought forth for the first time in the fall of 2009.